Int J Adv Manuf Technol (2017) 88:2621–2630
DOI 10.1007/s00170-016-8997-2

ORIGINAL ARTICLE

Deformation mechanism and performance improvement of spline shaft with 42CrMo steel by axial-infeed incremental rolling process

Min-Chao Cui[1] · Sheng-Dun Zhao[1] · Da-Wei Zhang[1] · Chao Chen[1] · Shu-Qin Fan[1] · Yong-Yi Li[1]

Received: 29 February 2016 / Accepted: 30 May 2016 / Published online: 4 June 2016

Abstract In this paper, a novel axial-infeed incremental rolling process of spline shaft with 42CrMo steel is proposed to solve the problems of present manufacture process. The principle of the axial-infeed incremental rolling process is introduced firstly, and then the deformation mechanism is analyzed by finite element method (FEM). The numerical results show that the deformation and material flow during the novel process only occurs in the surface layer of the blank, and the metal flow velocity component along the radial direction is significantly higher than that along the axial direction. Next, the experimental research is carried out on axial-infeed incremental rolling equipment, and the microstructure and hardness of the products are evaluated. The experimental results show that the microstructure in the surface of tooth profile, and root is fibrous tissue which is continuous, dense, and streamlined, and the hardness of the tooth profile and root area obviously increases.

Keywords Spline shaft · Axial-infeed incremental rolling process · 42CrMo · Deformation mechanism · FEM · Experiment

1 Introduction

Spline shafts are widely used to transmit motion or torque between shafts in the mechanical system, and the advantages of spline shaft connection attracted lots of interests attributed to their high connection strength, high reliability, compact structure, and convenient assembly [1]. The various advantages of spline shaft connection bring the extensive application of spline shaft in the industries of aerospace, ship, engineering machinery, and automobile. For instance, a common automobile contains about 30 spline shafts, and their installation positions include half shaft, clutch, differential, transmission, etc. [2]. Furthermore, higher requirement of the performance of spline shaft has been put forward in the modern manufacturing. Thus, it is essential to study the novel manufacture process of spline shaft to obtain higher performance.

Recently, the researches and applications of the plastic rolling process of spline shaft become more and more active for its advantages such as superior product quality, saving of raw materials, high productivity, and low cost [3–5]. Rolling process can be applied in the products which have axisymmetric cross area such as spline shafts and gears [6, 7]. The traditional rolling processes can be summarized as three types: rolling process with rack dies, with round dies, and with incremental dies. Figure 1 shows the principle of traditional rolling processes applied in spline shafts. The blank is just rotated along the circumferential by the driven of dies, and the teeth are formed in the radial direction gradually due to the in-feed of dies. Although these traditional rolling processes can realize the forming of spline shaft, there are still some problems such as the huge forming load, dies wear, inaccurate tooth number of formed spline shaft, and insufficient of material flow [4, 7]. In an attempt to solve the above problems, an axial-infeed incremental rolling process of spline shaft with 42CrMo steel is proposed. It is a novel metal forming process in which the blank of spline shaft is pressed into the rolling dies continuously and the material in the surface of the blank is formed to a certain shape (the principle is illustrated in Section 2). The forming load is divided into axial and radial load, so the die life improves. There are many factors that

✉ Min-Chao Cui
cuiminchao@163.com

[1] School of Mechanical Engineering, Xi'an Jiaotong University, No. 28 Xian Ning West Road, Xi'an, People's Republic of China

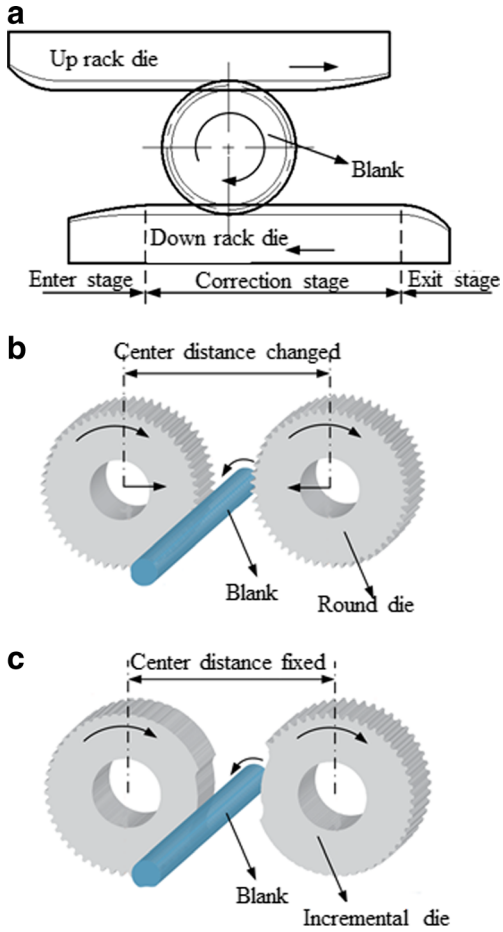

Fig. 1 The schematic diagrams of traditional rolling processes of spline shaft: **a** with rack dies, **b** with round dies, and **c** with incremental dies

affect the axial-infeed incremental rolling process such as die angle, in feed velocity and rotational speed, and the finite element method (FEM) is also widely utilized to optimize the process parameters [8, 9]. The plastic properties and constitutive equations of 42CrMo steel were investigated [10–12]. The experimental research on forming parameters for spline rolling with round dies was carried out [13]. The phase synchronous problem of three dies was solved by Zhang et al [14].

In this paper, the objective is to investigate the deformation mechanism during the axial-infeed incremental rolling process by FEM, and then the experimental research is carried out on axial-infeed incremental rolling equipment. Next, the microstructure of the cross section of formed spline shaft is observed and the performances of product are evaluated.

2 Principle of the axial-infeed incremental rolling process of spline shaft

As shown in Fig. 2a, the axial-infeed incremental rolling system mainly contains three rolling dies, back-drive center, and blank. The three rolling dies were assembled along the circumference evenly. Along the axial direction, each rolling die contains die angle part with the angle α_e and correction part, as shown in Fig. 2b. The function of die angle part is preforming for spline shaft, and the function of correction part is adjustment for tooth profile. The back-drive center has the same tooth profile parameters with spline shaft, so it could determine the initial phase of the rolling dies and ensure the die speed keep consistent.

The axial-infeed incremental rolling process was shown in Fig. 3, and it includes the following steps: (1) The blank is clamped by the former-drive center and the back-drive center. (2) The rolling dies rotate at the same speed and drive the blank rotate. (3) The blank is fed along the axial direction by the center and the deformation of the metal occurs on the surface of the blank. Under the action of multiple pre-rolling, the plastic deformation of the blank increase continually. Then, the preformed tooth profile is adjusted by the correction part. Due to pre-rolling and adjust-rolling, the dimension precision and surface quality increase. (4) After rolling, the rolling dies retract slightly along the radius direction and the formed spline shaft is pushed off along the inversion direction, the forming process end.

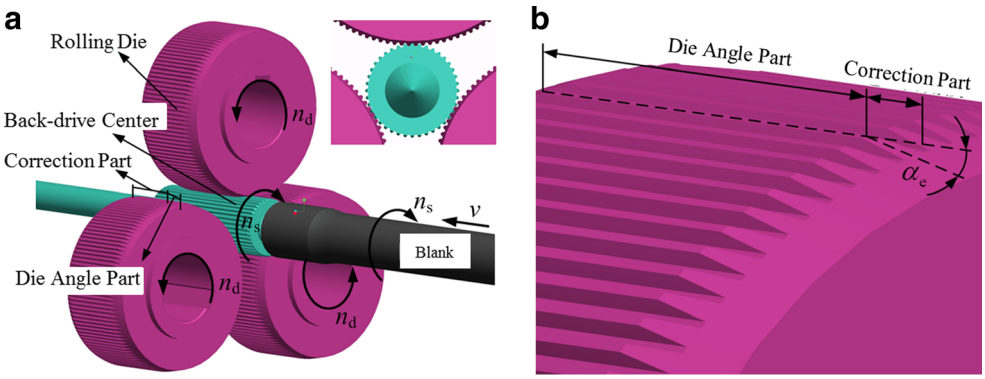

Fig. 2 Diagram of the axial-infeed incremental process: **a** the axial-infeed incremental rolling system and **b** the local structure of the rolling die

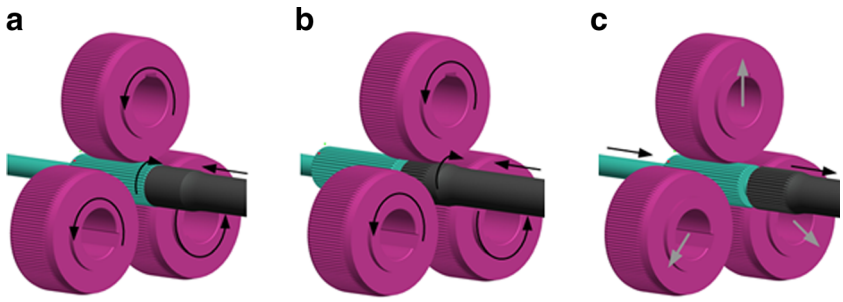

Fig. 3 Diagram of the steps of the rolling process: **a** before rolling, **b** during rolling, and **c** after rolling

3 Deformation mechanism analysis by finite element method

3.1 Finite element models and process parameters

The spline shaft investigated in this paper is derived from the half shaft of a heavy truck, and its blank diameter is calculated according to the principle of constant volume during the plastic forming process. According to the meshing theory, the tooth profile parameters of the rolling dies are the same as the parameters of the spline shaft [15]. Concisely, the parameters of the rolling dies and the blank are listed in Table 1.

Based on the DEFORE-3D software, the simplified finite element models of the axial-infeed incremental rolling process of spline shaft are established, as shown in Fig. 4a. Three rolling dies were assembled along the circumference evenly and the α_e of the rolling dies is set as 10°. The blank structure, constraints, and grid are shown in Fig. 4b. Along the axial direction, the blank is divided into three sections: a-tooth profile section, b-transition section, and c-connection section. The length of the tooth profile section is 32 mm. The connection section can be regarded as no-deformation, so the constraints of no-displacement in all direction are applied in connection section. Additionally, in order to increase the precision of finite element analysis, local mesh refinement is applied in the surface within the depth of 1.5 mm and the material characteristic of 42CrMo steel is obtained by isothermal compression tests at different strain rates.

The primal parameters of finite element analysis are as follows: the rotation speed of the rolling dies is 25 r min^{-1}, the rotation speed of the blank is 75 r min^{-1}, and the feed speed is 0.5 mm s^{-1}. The environment temperature is 20 °C, the heat convection coefficient between the models and the environment is 20 W m^{-2} °C^{-1}. The shear-based friction model is applied between the blank and the dies with the friction factor 0.12 [16].

By simulation, the tooth profile formation process of the spline shaft is shown in Fig. 5. In the early stage of the rolling process (t_r = 3 s), the blank is pre-formed by the rolling dies and its surface appears shallow tooth structure. In the middle and late stages of the rolling process (t_r = 3–25 s), the height of the tooth increases and the formed part become much longer along with the axial feed.

3.2 The equivalent stress distribution

Through the preliminary finite element analysis, Fig. 6a shows the equivalent stress distribution of the cross section in preformation area, which is apart from the entrance section 25 mm in the rolling process (t_r = 18 s). When the radius (r_p) is less than 15 mm, the equivalent stress is low (less than 200 Mpa). In the direction of OA (from the spline shaft center to the tooth addendum along the radial direction), it increases to 890 MPa as the radius r_p increases to 24.35 mm, but decreases from 890 to 820 MPa as the radius increases from 24.35 to 25.875 mm. In the direction of OF (from the spline shaft center to the tooth root along the radial direction), it increases with the increasing radius. It is notable that when the radius is greater than 23.5 mm, the equivalent stress rises sharply and reaches the maximum value 1240 MPa.

The equivalent stress distribution of the cross section in correction formation area, which is apart from the entrance section 20 mm, is shown in Fig. 6b. The characteristics of the equivalent stress distribution are almost same as the preformation area. But in the direction of OA, the equivalent

Table 1 Parameters of the rolling dies and the blank of spline shaft

Parameters	Value	Parameters	Value
Tooth number	120	Pitch circle diameter (mm)	150
Modulus (mm)	1.25	Root circle diameter (mm)	148.25
Pressure angle (degree)	30	Addendum circle diameter (mm)	151.3
Spline shaft length (mm)	40	Blank diameter (mm)	50.85

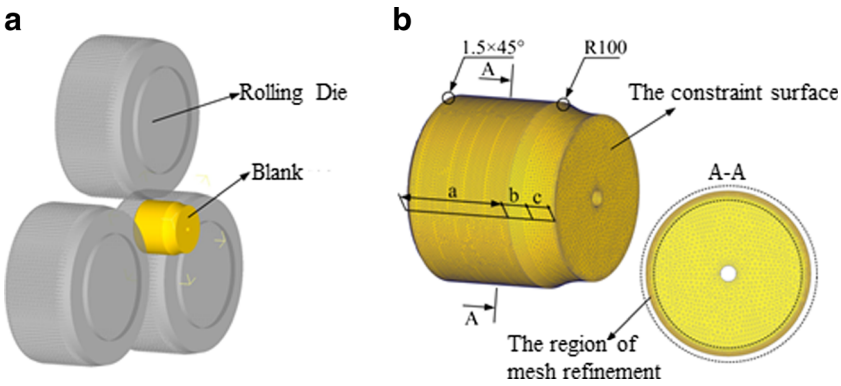

Fig. 4 Diagram of the finite element models: **a** finite element models and **b** the model of the blank

stress remarkably decreases when the radius increases from 24.35 to 25.875 mm and the minimum value is 776 MPa. In the direction of OF, it notably increases when the radius is greater than 23.5 mm and the maximum value is about 1725 MPa, which shows a different trend compared to the OA direction.

Consequently, the characteristics of equivalent stress distribution can be summarized as follows: The change of equivalent stress mainly concentrates on the surface of the spline shaft and the equivalent stress is almost zero at the center of spline shaft. The equivalent stress in tooth root is higher than in tooth addendum and in the correction formation area is higher than preformation area.

3.3 The equivalent strain distribution

The differences of the equivalent strain distribution reveal the accumulation of plastic deformation in plastic forming process. The larger the equivalent strain, the bigger the cumulative deformation. Also, the work hardening effect is remarkable and the surface quality as well as the fatigue strength tends to be better. Figure 7a shows the equivalent strain distribution corresponding to the different radii on cross section (axial distance 20 mm) of the final formed spline shaft. When the radius is less than 15 mm, it is negligible. In the direction of OA, it increases to about 7.24 as the radius increases to 23.5 mm, but decreases to about 5.06 (and stay around 5.06) as the radius increases from 23.5 to 25.875 mm. In the direction of OF, it increases with the radius increasing. Especially when the radius is greater than 23.5 mm, the equivalent strain rises sharply and reaches the maximum value about 12.57. In addition, the decline of the equivalent strain when the radius ranges from 23.5 to 25.875 mm in the direction of OA can be interpreted as, in the late rolling stage, the material in the middle and top of the tooth profile is extruded by the material in the tooth root and the bottom of the tooth profile, and moves freely along the outward radial direction. Therefore, the plastic deformation of material decreases at the late rolling stage (as shown in Fig. 7a).

Figure 7b shows the equivalent strain distribution (along the axial) in the surface layer ($r_p > 20$ mm) of the formed spline shaft. As shown, the deformation of the tooth root area is greater than the deformation of the tooth profile area on the arbitrary section, which is consistent with the deformation characteristics of the rolling forming process. In addition, the plastic deformation degree of tooth root and profile area decreases with the axial distance of the section increasing. This phenomenon can be interpreted as the correction cycles of the rolling dies decrease as the axial distance of section increases, so the plastic deformation degree decreases.

As a result, the characteristics of equivalent strain distribution can be summarized as follows: the plastic deformation mainly occurs on the surface layer of the spline shaft and the deformation degree decreases along the inward radial direction (almost no plastic deformation in the center of spline shaft). The deformation degree in the tooth root area is larger than that in the tooth profile area and it (both tooth root area and tooth profile area) decreases as the axial distance of section increases.

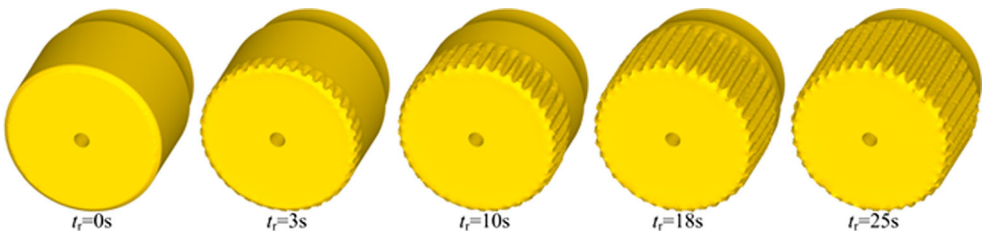

Fig. 5 Diagram of formation process of the spline shaft by FEM

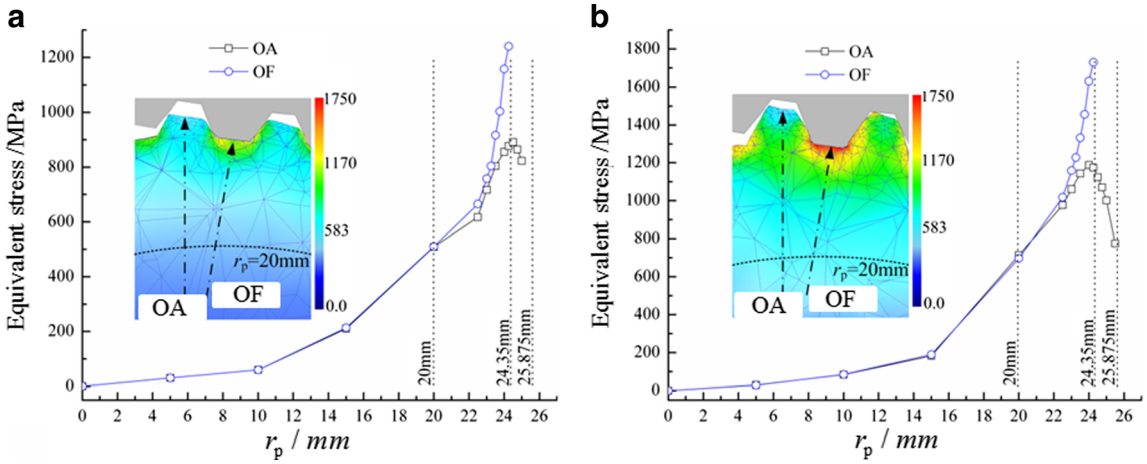

Fig. 6 The equivalent stress distribution of the spline shaft: **a** preformation area and **b** correction formation area

3.4 The behavior of material flow

Figure 8a shows the material flow velocity distribution of the spline shaft in axial-infeed incremental rolling process (t_r = 18 s). Material flow behavior is obvious viewed along the radial direction in preformed and correction formation area. According to the comparison between the radial and axial component of material flow in Fig. 8b, the metal flow velocity component along the radial direction is significantly higher than that along the axial direction, and this is favorable to the increasing of tooth of spline shaft in rolling process [17].

Figure 9 shows the material flow distribution in different section, and the longitudinal section is obtained from the tooth root area. On the section in the preformed area (axial distance d_c = 25 mm), the material in the tooth root area mainly flows along the radial inward direction, but the material in the tooth profile area mainly flows along the radial outward direction. On the section in the correction formation area (axial distance d_c = 20 mm), the material flow rate is lower than that in the tooth root area, but the characteristics of the material flow behavior are the same.

Figure 10 shows the comparison of the material flow displacement on different directions in the final formed spline shaft (the axial distance of the cross section is 20 mm). When the radius of spline shaft (r_p) is less than 20 mm, the displacement of material along the radial direction and the axial direction are basically equal. In the direction of OA, the displacement of material along the radial inward direction and axial direction increases as r_p increases from 20 to 23.5 mm, but decreases as r_p increases from 23.5 to 25.875 mm. Especially, when r_p is larger than 25 mm, the direction of material flow changes from radial inward direction to radial outward direction. At the top of tooth profile (r_p = 25.75 mm), the radial outward displacement of material (0.7 mm) is about 3.3 times of the axial displacement (−0.21 mm). In the direction of OF, the displacement along the radial inward direction and axial direction increases as r_p increases from 20 to 24.35 mm and the increasing trend is

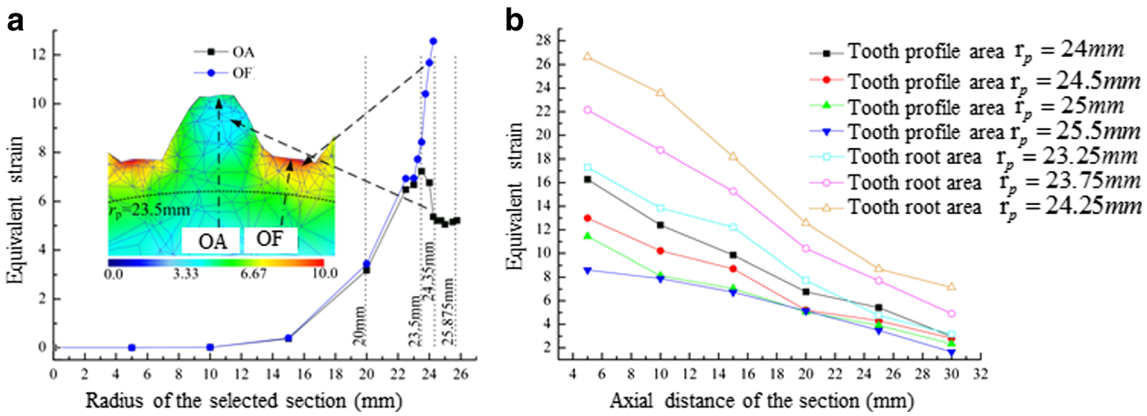

Fig. 7 The equivalent strain distribution of the formed spline shaft: **a** distribution along the radial direction and **b** distribution along the axial direction

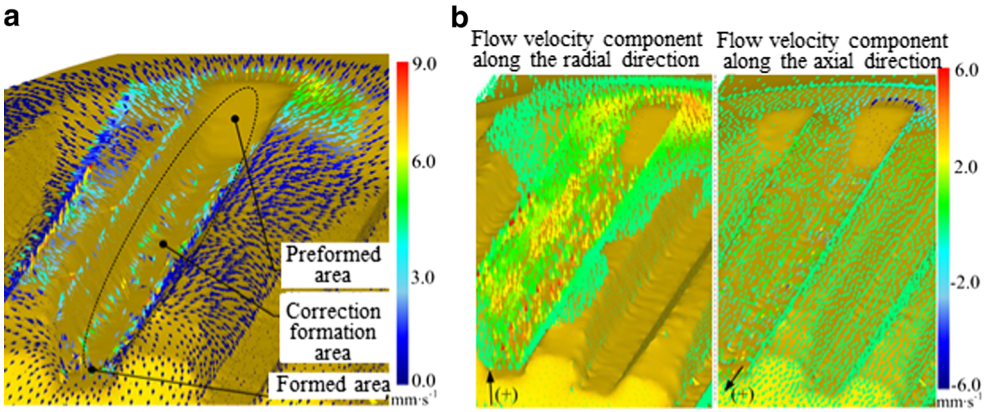

Fig. 8 The material flow velocity distribution of the spline shaft: **a** the distribution of material flow velocity and **b** the distribution of material flow velocity along different directions

more remarkable when r_p larger than 23.5 mm. At the bottom of tooth root (r_p = 24.25 mm), the radial inward displacement (−0.98 mm) is about 1.4 times of the axial displacement (0.71 mm).

Consequently, the behavior of material flow can be summarized as follows: the material flow mainly occurs in the surface layer of the spline shaft and almost no material flow in the center of spline shaft. In the tooth profile area, the flow of material along the radial outward direction is more obvious. But in the tooth root area, the flow of material along the radial inward direction and two side direction is more remarkable.

4 Performance improvement of spline shaft with 42CrMo steel after the novel process

4.1 Experiments and results

The axial-infeed incremental rolling equipment was designed, manufactured, and assembled as shown in Fig. 11. The axial movement of blank is realized by two air cylinders. The big one is installed in the right side and drives the former-drive center (not draw in Fig. 11). The small one is installed in the left side and drives the back-drive center (in the center of Fig. 11). When the bland feeding, the big cylinder provides propulsion and the small cylinder provides a proper clamping force. The axial forming force and friction force are overcome by the propulsion of big cylinder. When the blank exiting, the small cylinder provides a proper force to push-out the formed spline shaft.

Then, the experiments of axial-infeed incremental rolling process of spline shaft with 42CrMo steel are carried out and the metal structure and hardness of formed spline shaft are investigated.

The experimental blank of spline shaft is designed, which is similar to the finite element model in Section 3, and the shape and sizes are shown in Fig. 12a. Figure 12b is the real picture of the blank of spline shaft.

The axial-infeed incremental rolling experimental process is shown in Fig. 13. The whole rolling process lasted about 2 min, including (1) feed before rolling 15 s, (2) axial-infeed rolling 64 s (the feed speed v = 0.5 mm s^{-1}), (3) correction rolling 15 s, and (4) reverse out 15 s.

Figure 14 shows the formed spline shaft of FEM and experimental result of the axial-infeed incremental rolling process. It can be seen that the shape of FEM result shows a good

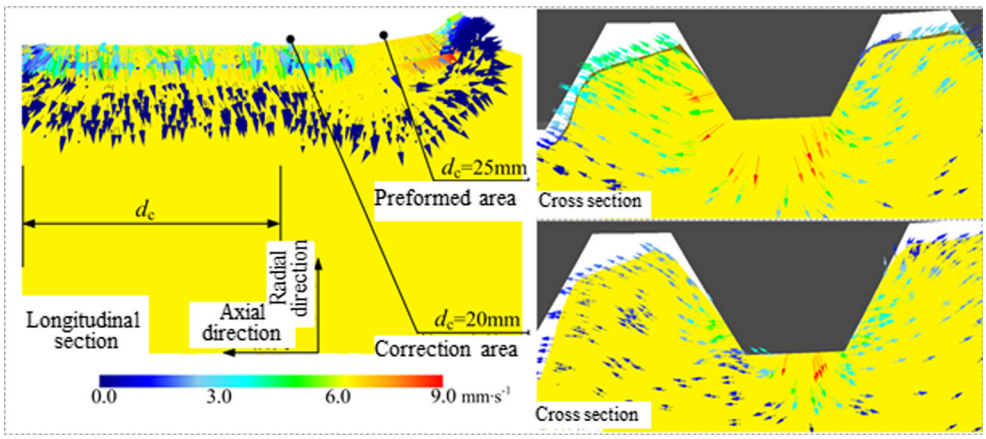

Fig. 9 The distribution of material flow in different sections

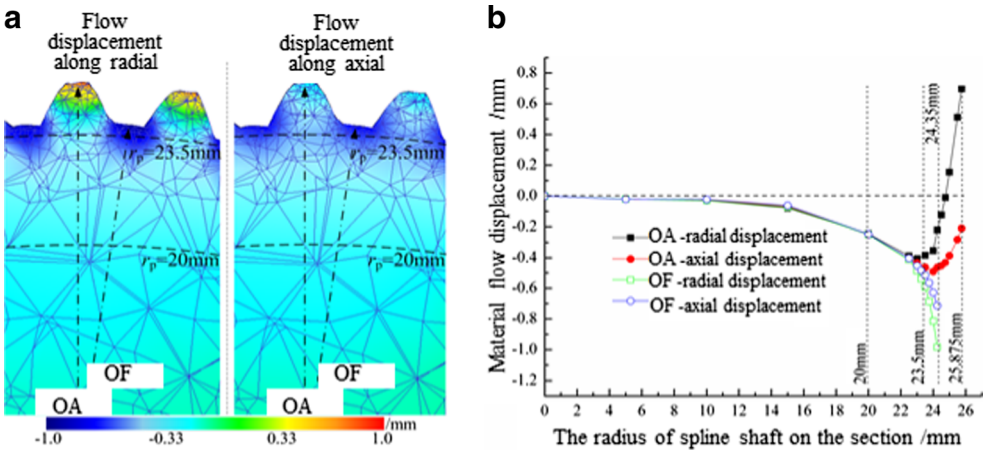

Fig. 10 The comparison of the material flow displacement on different directions in the final formed spline shaft: **a** material flow displacement nephogram and **b** compare of flow displacement

agreement with the experimental. Thus, it indicates that the finite element analysis of the novel process in Section 3 is credible.

4.2 The change of microstructure of the formed spline shaft

The microstructure of the formed spline shaft with 42CrMo steel is shown in Fig. 15 (the process parameters are the diameter of blank is 50.85 mm, the rotation speed of rolling dies is 25 r min^{-1}, the feed speed is 0.5 mm s^{-1}, the forming temperature is 20 °C, and the die angle of rolling dies is 9°). For details, the width of the sample is about 12 mm along the circumferential direction and the depth is about 10 mm along the radial direction. The sample is cut, polished, and corroded by 4 % nitric acid alcohol solution, and then it is observed by optical microscope (Leica DMI3000M metallographic microscope).

The microstructure contains ferrite, pearlite, and sorbite in the core and middle of the formed spline shaft, and the microstructure is slightly stretched along the outward radial direction in the bottom and top of the tooth profile (this change can evidently refine the grain size and improve the distributed uniformity of structure). The microstructure in the bottom of tooth root area is fibrous tissue which is composed of ferrite and pearlite. The fibrous tissue was refined obviously, and its flow line was distributed along the bottom of the tooth root to adjacent tooth root area, continue to the surface of tooth profile. The fracture, fragmentation, dissolution, balling of pearlite, and the refinement of ferrite are obviously viewed in this area, so the grain density increases. The surface of tooth profile is fibrous tissue which is composed of clipper-built ferrite and pearlite. The fibrous tissue's grain is obviously refined and dense, and the flow line is distributed along the direction of the tooth surface (With the increase of depth along the direction from the tooth surface to core, the fibrous tissue disappears gradually, and the grain density reduces gradually).

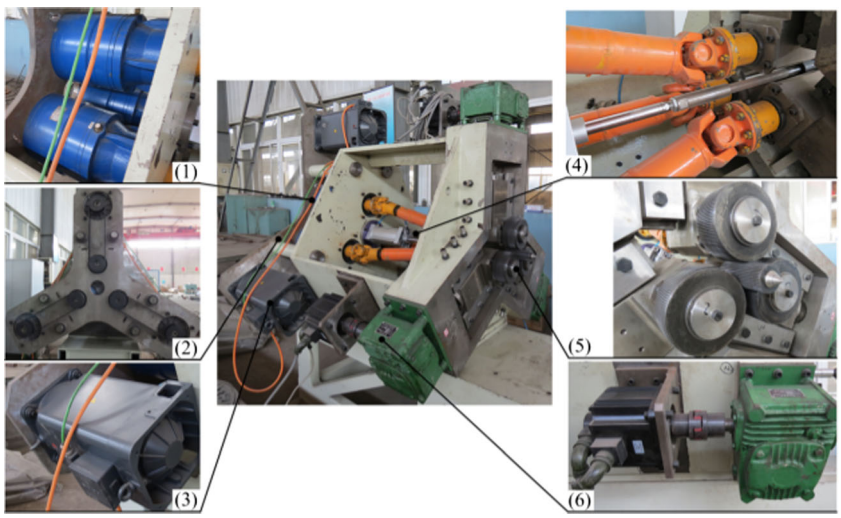

Fig. 11 The axial-infeed incremental rolling equipment: (*1*) planetary reducer, (*2*) synchronous belt transmission, (*3*) main AC servo motor, (*4*) universal coupling, (*5*) rolling position, and (*6*) diameter control AC servo motor and worm gear reducer

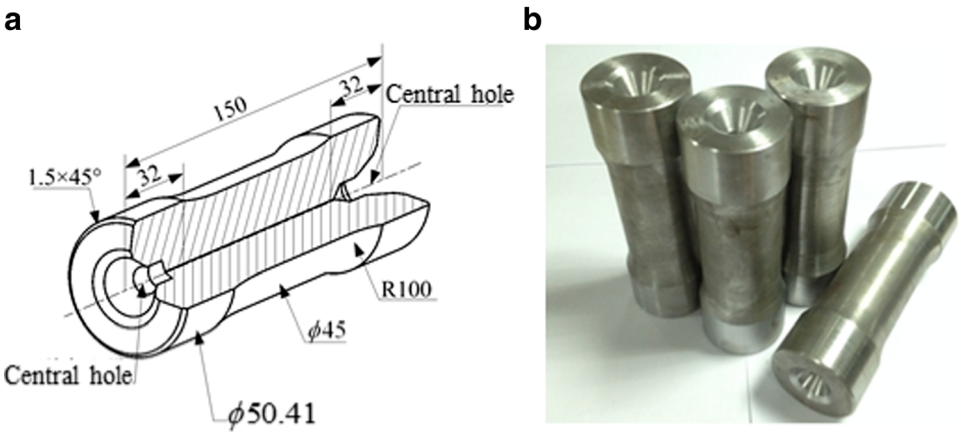

Fig. 12 The shape and sizes of the blank of spline shaft: **a** shape and sizes and **b** real picture

4.3 The change of hardness of the formed spline shaft

In order to investigate the change of hardness of the formed spline shaft, the hardness of different areas on the section of spline shaft was measured and analyzed (HV standard). Considering the original differences of the spline shaft, the measurement scheme is shown in Fig. 16a. There are three areas (I, II, and III), which are 120° apart, on the section measured, respectively, and seven different positions (P1–P7) are measured in each area.

The HV hardness value in the three measured areas presents the same trends as shown in Fig. 16b. The organization of the core of spline shaft is unchanged, so the hardness values are similar at P1 and P2 (about 230). The organization of the bottom of tooth profile is slightly elongated and refined, so the hardness value slightly increases (about 245 at P3). The hardness value of the core of tooth profile slightly decreases (about 238 at P4). The organization of the surface of tooth profile is fibrous tissue which is continuous, dense, and streamlined, so the hardness value obviously increases (about 300 at P5). The hardness value of the tooth root area (P6) has little change relative to the tooth surface area (P5), and the value is about 290 at P6. The organization of the bottom of the tooth root is more dense and continuous, so the hardness value increases at P7 (about 310). The increase of tooth profile and root area improves the hardness and the fatigue strength of spline shaft. It can be concluded that the characteristics of the hardness distribution of spline shaft are consistent with the characteristics of the cumulative plastic deformation distribution in numerical simulation, and this indicates that there is obvious work hardening effect in tooth profile and root area. As a result, the axial-infeed incremental rolling process can improve the organization and performance of spline shaft, and it realizes the integration manufacturing and forming of spline shaft.

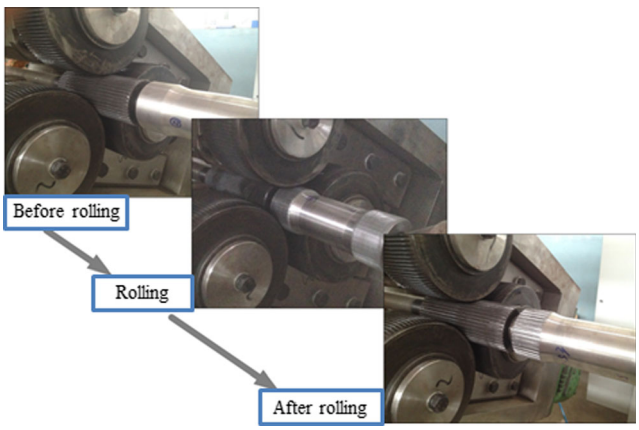

Fig. 13 The axial-infeed incremental rolling experimental process

5 Conclusion

Through the above studies on the axial-infeed incremental rolling process, the conclusions are listed as follows:

(1) The change of equivalent stress mainly concentrates on the surface of the spline shaft during the axial-infeed incremental rolling process of spline shaft. The equivalent stress in tooth root is higher than in tooth addendum and in the correction formation area is higher than preformation area.

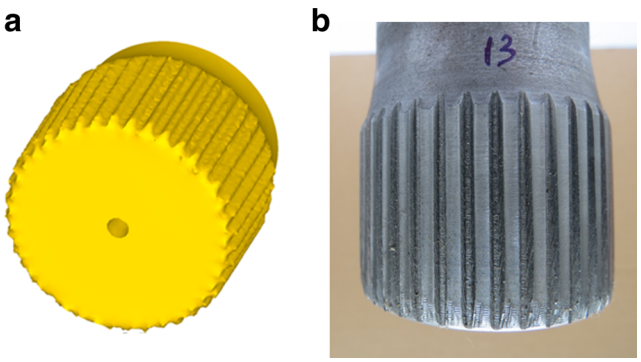

Fig. 14 The formed spline shaft: **a** FEM result and **b** experimental result

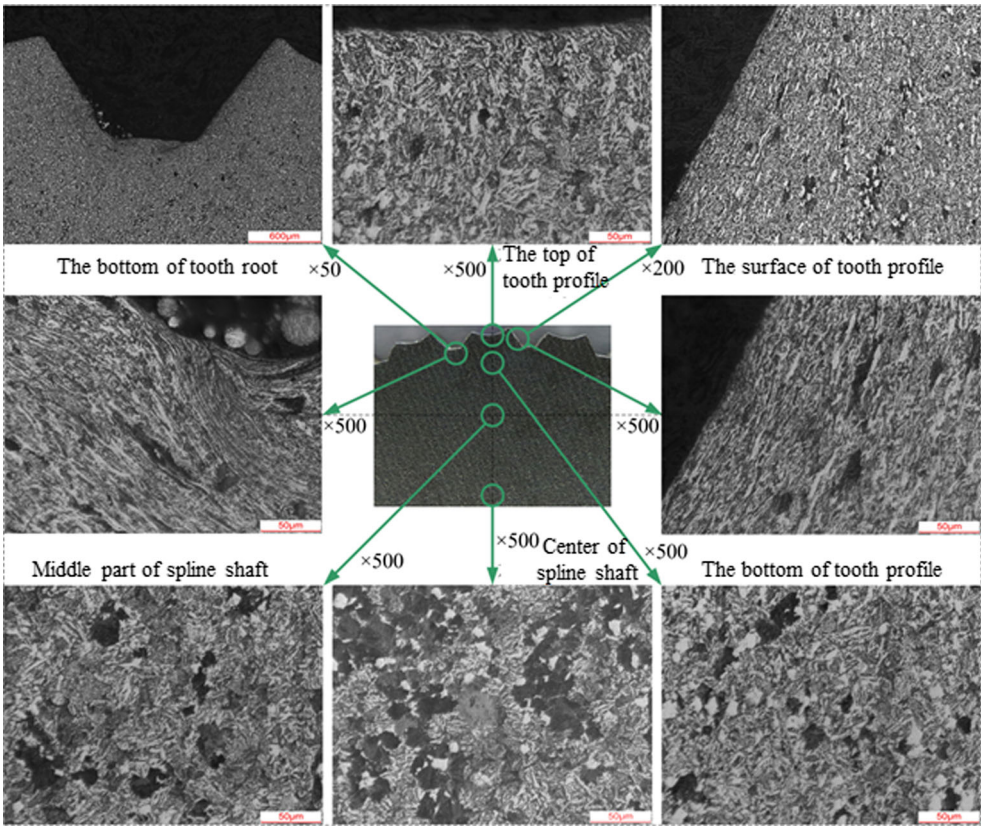

Fig. 15 The metal structure of the formed spline shaft with 42CrMo steel

(2) The plastic deformation mainly occurs on the surface layer of the spline shaft, and the deformation degree decreases along the inward radial direction. The deformation degree in the tooth root area is larger than that in the tooth profile area and it (both tooth root area and tooth profile area) decreases as the axial distance of section increases.

(3) The material flow mainly occurs in the surface layer of the spline shaft and almost no material flow in the center of spline shaft. In the tooth profile area, the flow of material along the radial outward direction is more obvious. But in the tooth root area, the flow of material along the radial inward direction and two side direction is more remarkable.

(4) The microstructure in the surface of tooth profile and root is fibrous tissue which is continuous, dense, and streamlined, and the hardness of the tooth profile and root area obviously increases. Thus, the axial-infeed incremental rolling process can realize the integration manufacturing and forming of spline shaft.

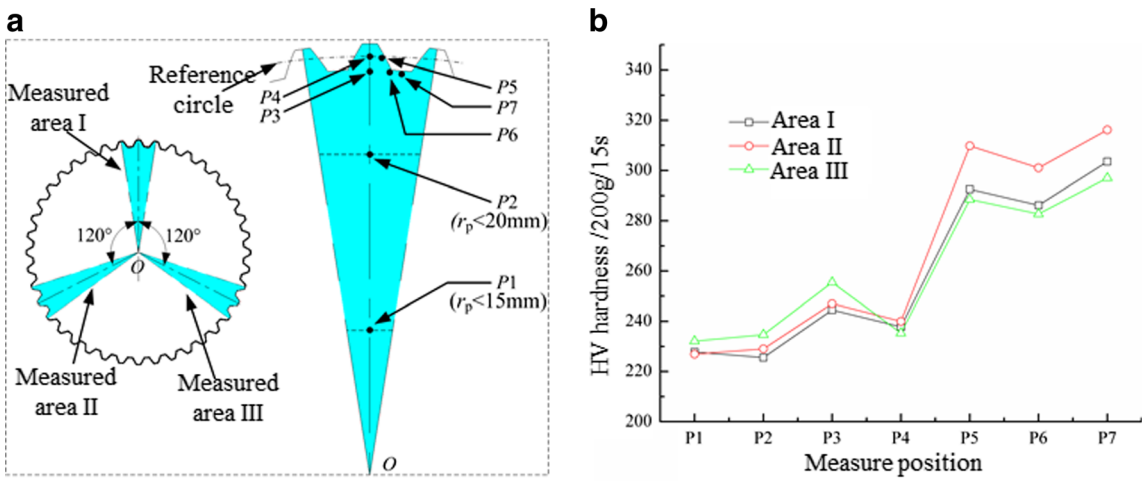

Fig. 16 The HV hardness measurement scheme and results: **a** the measurement scheme and **b** the measure results

Compliance with ethical standards

Funding The authors gratefully acknowledge the contribution of the subjects: National Natural Science Foundation of China for key Program (Grant No. 51335009), Shaanxi Province Natural Science Foundation of China (Grant No. 2014JQ7273), and State Key Laboratory for Mechanical Behavior of Materials (Grant No. 1991DA105206).

References

1. Li YY, Zhao SD, Fan SQ, Yan GH (2013) Study on the material characteristic and process parameters of the open-die warm extrusion process of spline shaft with 42CrMo steel. J Alloys Comp 571: 12–20
2. Zhang DW, Li YT, Fu JH (2007) Mechanics analysis on precise forming process of external spline cold rolling. Chin J Mech Eng-En 20:54–58
3. Neugebauer R, Klug D, Hellfritzsch U (2007) Description of the interactions during gear rolling as a basis for a method for the prognosis of the attainable quality parameters. Prod Eng Res Devel 1:253–257
4. Zou L, Xia JC, Wang XY, Hu GA (2003) Optimization of die profile for improving die life in the hot extrusion process. J Mater Process Technol 142:659–664
5. Lee RS, Sheu JJ, Gau YJ (1991) Optimum die-surface design of gear-spline extrusions using a general surface model. J Mater Process Technol 28:365–382
6. Neugebauer R, Putz M, Hellfritzsch U (2007) Improved process design and quality for gear manufacturing with flat and round rolling. Ann CIRP 56(1):307–312
7. Zhang DW, Zhao SD (2014) New method for forming shaft having thread and spline by rolling with round dies. Int J Adv Manuf Technol 70:1455–1462
8. Kao YC, Cheng HY, She CH (2006) Development of an integrated CAD/CAE/CAMsystemon taper-tipped thread-rolling die-plates. J Mater Process Technol 177:98–103
9. Domblesky JP, Feng F (2002) A parametric study of process parameters in external thread rolling. J Mater Process Technol 121: 341–349
10. Quan GZ, Tong Y, Luo G, Zhou J (2010) A characterization for the flow behavior of 42CrMo steel. Comput Mater Sci 50:167–171
11. Lin YC, Chen MS, Zhang J (2009) Modeling of flow stress of 42CrMo steel under hot compression. Mater Sci Eng A 499:88–92
12. Li YY, Zhao SD, Fan SQ, Zhong B (2013) Plastic properties and constitutive equations of 42CrMo steel during warm forming process. Mater Sci Technol 30(6):645–652
13. Liu ZQ, Song JL, Qi HP, Li YT, Li XD (2010) Parameters and experiments on the precision forming process of spline cold rolling. Appl Mech Mater 34–35:646–650
14. Zhang DW, Zhao SD, Wu SB, Zhang Q, Fan SQ, Li JX (2015) Phase characteristic between dies before rolling for thread and spline synchronous rolling process. Int J Adv Manuf Technol 81: 513–528
15. Huang ZH, Fu PF (2001) Solution to the bulging problem in the open-die cold extrusion of a spline shaft and relevant photo plastic theoretical study. J Mater Process Technol 114:185–188
16. Altinbalik T, Ayer Ö (2008) A theoretical and experimental study for forward extrusion of clover sections. Mater Des 29:1182–1189
17. Rezaei Ashtiani HR, Parsa MH, Bisadi H (2012) Constitutive equations for elevated temperature flow behavior of commercial purity aluminum. Mater Sci Eng A 545:61–67